MEER-iREC

Mirrors for Earth's Energy Rebalancing
-An inclusive Research Education Community
For Climate Adaptation and Mitigation

INTRODUCTORY MANUAL (2022-2023) &
STANDARD OPERATING PROCEDURE (SOP)

LEAD PARTICIPANTS:

Thomas Reis (Austria)

Glenn Ferguson (Canada)

Panagiotis Protsonis (Greece)

Satish V. Patil[a] (India)

Jasna Grabic[b] (Serbia)

Jay Johnson (USA)

[a]North Maharshtra University

[b]University of Novi-Sad

The MEER Framework

December 6, 2022

Contents

1 Participants Contact Information

Glenn Ferguson Citizen Scientist
1888 Mabou Road
Port Hood, Nova Scotia
B0E 2W0 Canada
ovkayak@gmail.com
p: 1-819-329-7843

Jasna Grabić Associate Professor
University of Novi Sad
Faculty of Agriculture
Department of water Management
Trg D. Obradovica 8
21000 Novi Sad, Republic of Serbia
jasna.grabic@polj.uns.ac.rs

Jay Johnson Science Teacher
Eagle Ridge High School
677 S 7th Street
Klamath Falls, OR 97601
jamesjohnson19841@moreland.edu

Satish V. Patil Associate Professor
North Maharashtra University
Jalgaon, India
satish.patil7@gmail.com

Panagiotis Protsonis Citizen Scientist
Perikleous Street 10
Selianitika Aigialeias
TK 25100 Achaia Greece
pitprots1@protonmail.com
p: +30 699 497 1000

Thomas Reis Renewable Energy Engineer
Off-Grid.at GmbH
Am Steinfeld 6
2511 Pfaffstätten, Austria
thomas.karl.reis@gmail.com
p: +43 2252 256 361

2 MEER Faculty Contact Information

Lisa Doner Associate Professor
Plymouth State University
17 High Street, MSC 48
Plymouth, NH 03264-1595
ladoner@plymouth.edu
p: 603 535 3180

Eric G. Hoffman Professor
Plymouth State University
17 High Street, MSC 48
Plymouth, NH 03264
ehoffman@plymouth.edu
p: 603 535 2321

Tracey Lesser Program Coordinator/Professor
NHTI-Concord's Community College
31 College Drive
Concord, NH 03301
tlesser@ccsnh.edu
p: 603 271 6484 x 4423

Ye Tao Funder and Director
The MEER Framework
23564 Calabasas Road, Suite 201
Calabasas, CA 91302
tao@rowland.harvard.edu

3 Executive Summary

Climate change initiated by anthropogenic carbon pollution is now a major threat to human civilization and ecosystems [1, 2]. As climate stressors intensify, adaptation and mitigation increasingly involve transition to a low-energy economy at the local community level [3]. Technologies to enable this transition are still in early stages of development and policy at levels from local to national are disordered and inconsistent [4, 5]. Given the urgency, successfully achieving resilience requires developing and sharing the science and technical knowhow widely, as they emerge in realtime. The purpose of the present document is thus to widely disseminate, among citizen scientists and school outreach participants, the technical knowhow MEER has so far gleaned through prototyping and using our first-generation devices based almost exclusively on glass.

At the community-level, a key challenge to resilience is food security and self-sufficiency because of increasingly severe and frequent heatwaves and droughts [6, 7, 8, 9, 10, 11, 12, 13]. Heat exacerbates drought by accelerating evaporation and transpiration [14, 15, 16, 17, 18]. Increasing temperatures in Winters and during snow melting seasons is also contributing to decreasing planetary albedo and altering ice phenology and exerbating the rate of warming [19, 20]. This project takes on these multiple challenges, employing cutting edge technology to test the feasibility of using near-ground-level mirrors to reflect away a small percentage of incoming solar radiation before it can be absorbed and re-radiated as greenhouse gas-reactive infrared energy. We examine, at a very small scale, the impacts of individual mirrors and microarrays on local conditions in order to better anticipate the climate and environmental impact of large scale deployment. An equally important goal is to use the system for local capacity building around the world, in science, technology, and pedagogy.

Solar radiation management essentially controls conversion of shortwave solar radiation into heat. Theoretically, it reduces thermal energy flux through plants and soils, consequently reducing ground temperatures and evaporative water loss. Despite this conceptual simplicity, there are no publications reporting experimental results on the impact that mirror arrays have on the micro-environments around them. MEER teams at Plymouth State University (PSU) and at the New Hampshire Technical Institute (NHTI) are currently conducting systematic experimental investigation of the abiotic and ecosystem responses to mirror arrays as a function of surface coverage by mirrors, and of the differential impact of various glass materials. In this multi-institution collaboration, investigators with expertise spanning climate physics, ecology, chemistry, material science, mechanical engineering, and social sciences collaborate to comprehensively examine the physical and biological impacts of glass mirror arrays on the local environment. Specifically, we explore the response of soil temperature, water content, air temperature, air humidity, radiation flux, wind speeds, as well as plant growth rate and physiology.

Alongside the main field experiments, we address a grand challenge in education, bringing technology into the reach of diverse, often underserved populations and communities around the globe, including rural sectors. We do this through open education resource sharing, direct outreach to K-16 and public audiences, the development of demonstration kits and education modules, and building towards the world's first multidisciplinary inclusive Research Education Community (iREC) [21, 22, 23]. The experimental prototypes described in this manual can be used over multiple years, with varying methods for data acquisition, for investigating different environmental questions, and over different ground types, urban, natural, and agricultural. The concept can be easily adopted for formal and informal educational purposes worldwide, and lead to scientific data worthy of publication. We therefore expect individual local projects to inspire community-level, grass-roots science and citizen engagement and to instill hope for solving one of humanity's biggest challenges around climate change.

4 Introduction and Motivation

4.1 Climate change and its impacts

As a result of anthropogenic carbon releases to the atmosphere, Earth has entered a state of positive energy imbalance unprecedented, in the planet's geologic history, by the rate of warming. The imbalance is characterized by the storage of ocean and atmospheric heat at 400 Terawatts [24, 25, 26, 27, 28], twenty times more than the human civilization energy dissipation rate. This imbalance has driven a warming trajectory now known as anthropogenic climate change, or global warming [29]. Researchers across many scientific and social science disciplines, plus the general public, are increasingly alarmed by this phenomenon. It is primed to induce, within the lifetimes of most of the planet's human population, a massive scale of global suffering through extreme-weather events, heat strokes [6, 8, 30], drought and crop failure [12, 13, 31, 32, 33], internal displacement [34, 35], ecosystem collapse [1, 36, 37], and, less intuitively, armed conflict [2], pandemics [38, 39, 40], and suicide [41].

4.2 Mechanism of ecosystem collapse

Climate change impacts are predominantly due to the sensitivity of biological processes to heat, leading to decay of fitness for most lifeforms, including important food crops and fisheries [42, 43, 44, 45], with intensifying heatwaves and droughts [7, 46, 47, 48, 49, 50]. Biological fitness has a peak optimal temperature, and a range of tolerance around the peak. Fitness falls sharply as temperatures rise to several degrees above the optimum [46, 51, 52, 53, 54]. Species and subpopulations can have different optimal temperatures and optimal temperature ranges, usually matching conditions in their native environments [55]. The fitness curves are asymmetric with respect to temperature such that many organisms show more sensitivity to, and harm from, overheating than overcooling [56]. A temperature increase of 2-3°C above historical habitat conditions consistently induces local extirpation [57, 58, 59], ecosystem regime shift and collapse [1, 36, 37, 60].

4.3 We have committed to warming beyond 2°C

In 2020, key climate parameters were recently reassessed [61, 62], and they paint a much bleaker future than implied by previous reports by the Intergovernmental Panel on Climate Change (IPCC) [63]. When the most advanced climate models (CMIP6) were updated with new understanding of cloud and aerosol mechanisms, Earth's transient climate response (TCR) jumped to 2.0 ± 0.4°C per CO_2 doubling [1], the high extreme of earlier predictions (0.8-2.5°C) [62, 64]. TCR refers to the rapid change in Earth's surface and ocean mixed layer temperature, on the time scale of years, following a step-function perturbation in heating power. At the same time, equilibrium climate sensitivity (ECS), supported by multiple lines of evidence, increased from

[1] Equivalent to 3.7 W m^{-2} of radiative forcing.

1.5-4.5°C to 2.4-4.5°C per CO_2 doubling [61, 65]. ECS involves the slower processes of vegetation and land ice changes and so predicts conditions over a time scale of centuries [66, 67]. The new TCR range agrees with the 1.3°C of actual warming that has occurred so far, from a net radiative forcing of 2 W m^{-2} [68, 69]. It now appears improbable that even an immediate highly unlikely cessation in anthropogenic fossil fuel emissions will prevent global average temperatures from exceeding 1.5°C because about 1.2 W m^{-2} of radiative forcing are temporarily suppressed by aerosol co-emitted during fossil fuel burning [61, 70, 71, 72, 73, 74, 75, 76, 77]. The new TCR estimate points to *an additional* ≈ 0.7°C increase and the new ECS range implies that as yet unrealized heating from Earth's energy imbalance will inevitably bring us above 2°C [29, 78, 79, 80, 81, 82, 83, 84, 85]. This is extremely bad news given existing and accumulating knowledge about ecological and agricultural vulnerability, and demonstrates that climate mitigation is an urgent priority for humanity. This proposal describes experiments with mirror arrays designed to explore avenues for climate mitigation.

5 Proposed Research

We share experimental kits with researchers, educators, students, and community members around the world who seek to understand and teach key principles of climate change physics and mitigation possibilities via micro-environmental solar radiation engineering. All participants agree to collaborate with each other and with MEER by co-developing and openly sharing data, technical engineering advances, custom data analysis softwares, and open educational modules for use with the experimental kits, including ideas for hands-on-learning-through-experimental-discovery, hypothesis testing and make-it-yourself ideas for students to do in class settings or at home.

Globalization of research and education outcomes will be promoted through publication of peer-reviewed articles, of teaching module and design concept in open education journals, presentations at international conferences and development of a free, themed media series with sharable links posted on MEER.org and instructions in multiple languages. This project also creates opportunity to learn about public reactions to mirror arrays, and to test the influence of outreach in changing attitudes/acceptance of these kinds of climate mitigation efforts, thus linking this STEM-focused project to the social sciences. Similar work has been done to assess the impact of windfarms [86] and solar energy farms [87] on viewsheds.

The experimental project presented here is based around a research question that asks "How feasible and how effective is climate adaptation using a ground-based array of mirrors to reflect away some of the incoming solar radiation (visible light) that would otherwise be absorbed and reradiated to interact with greenhouse gases?" The feasibility question is complex and involves many practical details, including materials costs, labor, impact on landscapes, infrastructure durability, and social acceptance of the presence of mirror arrays in addition to the actual climate impact. The effectiveness question requires a precise quantification of local ecological, primary productive, albedo, hydrological, and economic cobenefits. Because of these factors, a minimum array size is most desirable; this is because expansion of scale should improve both feasibility, by dropping unit cost, and effectiveness, by exploiting collaborative cooling effects of neighboring infrastructures.

Thus, a corollary question is "What is the minimum area of mirrors needed to have a measurable microenvironmental or climate effect?" We approach these research questions through replicate pilot tests from an individual-device scale to a micro-array scale, roughly 10 m^2 each, with albedo and structural controls enabled by black glass and transparent glass, respectively. The experimental design thus enables data collection for evaluating the effectiveness of the mirrors in creating ecologically diverse microclimates in their immediate vicinity, is a necessary predecessor step to implementation of the global climate mitigation idea, and importantly will not generate any unforeseeable, negative global impact due to its vanishing scale.

The device deployed for the current cycle of experiments are based almost entirely on glass as both the structural and functional material. A advantage of glass devices is their durability against corrosive degradation, once optimally designed and installed. An important drawback of glass is its weight, making shipping of material challenging, especially at small scales. Another drawback is risk of catastrophic failure and debris generation in the case of severe hail storms and tornados. Future iterations of the experiment will feature more light-weight materials based on hybrids among glass, bamboo, plastics, and sparing use of recycled metals.

In the following subsections, we describe examples of specific research questions that can be addressed with the common set of mirror and glass devices.

5.1 Soil cooling and moisture retention

This study is suitable for most regions around the world and specifically examines the impact of the mirrors on net energy flux at the surface, manifested by changing temperature and moisture of the soil in the ground and of the air right above it; in other words, the micro-environments around the mirrors, and the effects of shading and cover created by the presence of the mirrors. We investigate multiple land surface types, from soil in rural, agricultural environments, to concrete and asphalt surfaces characterizing urban environments, to frozen permafrost, mountain snow cover, and glaciers. We anticipate several outcomes from the proposed experiments and test these with null hypotheses:

Prediction 1.1: The presence of the mirrors will create a micro-environment under the arrays manifested by cooler ground and soil temperatures during periods of high solar irradiance, and greater soil moisture, and these effects will scale proportionally to the temporal coverage by shadows projected by the mirrors and black glass (Fig. 1). **$\mathbf{H}_0$(1.1) null**: There is no measurable difference in ground temperature, that systematically varies with location of the soil with respect to mirror placement and shadow sweep regions.

If **$\mathbf{H}_0$(1.1)** is false, then

Prediction 1.2: The shading of direct radiation by individual mirrors create significant micro-scale spatial heterogeneity in ground temperature within each array (Fig. 2). **$\mathbf{H}_0$(1.2) null**: Soil temperature is uniform around any single device.

Prediction 1.3: A 20°, South-facing tilting geometry of each mirror device during the warmer half of the year (see Section 8) directs precipitation towards one side of the mirror, increasing soil moisture under the southern edge of an individual mirror, compared to in other micro-environments (Fig. 2). **$\mathbf{H}_0$(1.3) null**: Soil moisture is uniform to within background experimental variability around any single device.

Prediction 1.4: The micro-environmental impacts observed for mirrors are similar to but measurably different compared to those due to black glass devices. Specifically, we predict increased rate of desiccation of soil underneath the black glass as compared to under mirrors. The moisture is still higher compared to control. **$\mathbf{H}_0$(1.4) null**: Soil moisture measured around black glass devices are not measurably different from those measured at corresponding microenvironments under mirror devices.

Prediction 1.5: Transparent glass devices create measurable micro-environments by attenuating solar radiation, modifying the IR radiation environment at night, and perturbing wind profiles. Impacts are smaller compared to those under mirrors and black glass. $\mathbf{H_0}$**(1.5) null**: Soil moisture measured around transparent glass devices are not measurably different from those arising from natural, lateral variability in the soil.

Analysis and meaningful interpretation of the soil data requires data on other environmental variables that will be studied by a project focusing on atmospheric conditions (Section 5.2).

5.2 Air temperature and air moisture

This study should be implemented at the same time as the soil/ground study and specifically examines the impact of the mirrors on atmospheric parameters, including air temperature, humidity, and energy balances in the layer of air between ground and the device as well as right above the latter; in other words, the above-ground micro-environments both under and above the mirrors via the effects of shading and cover created by the presence of the mirrors and other glass devices, as well as altered radiation-heat conversion and convective heat transfer. The aim is to qualitatively characterize changes to the fluxes of sensible heat (through air temperature) and latent heat (through air humidity) in and near the devices.

Multiple air temperature and humidity sensors will be installed within each experimental plot. Data on air temperature, relative humidity, and incoming visible light will come from continuous monitoring by sensors located at strategically chosen positions within each array. We anticipate several outcomes from the proposed experiments and test these with null hypotheses:

Prediction 2.1: The presence of the mirrors and glass plates will create above-ground micro-environments within and around the mirror arrays manifested by cooler air temperatures compared to the control, and this effect will be more prominent in a 2x2 array compared to under a single device (Fig. 2). $\mathbf{H_0}$**(2.1) null**: There is no measurable difference in air temperatures between the control plot and any of the plots with glass arrays.

If $\mathbf{H_0}$**2.1** is false, then

Prediction 2.2: Air temperature displays heterogeneity around the mirror devices, manifested by the lowest temperature below the mirrors in air volumes directly shadowed by a mirror around solar noon, higher in the air space shielded from direct solar radiation and below the installation height of mirrors, and highest at elevations above the mirrors. The relative trend between above- and below-device measurements reverse during the night. Generally, diurnal temperature amplitude is attenuated underneath the devices and in the shade, relative to control. $\mathbf{H_0}$**(2.2) null**: There is no measurable difference in air temperatures at various heights and lateral locations within each mirror array.

If $\mathbf{H_0}$**2.1** is false, then also

Prediction 2.3: Air temperature displays heterogeneity around the black glass devices, manifested by the lower temperature below the glass in air volumes directly shadowed by a plate around solar noon (micro-environment *d*, Fig. 2), higher in the air space shielded from direct solar radiation and immediately below the installation height of mirrors, and highest directly above the black glass. The air temperature above the black glass is higher than control values. The relative trend between above- and below-device measurements reverse during the night. The average temperature is higher than underneath mirror devices and amplitude attenuation is also less than under mirror devices. **H_0(2.3) null**: There is no measurable difference in air temperatures at various heights and lateral locations within each black glass array.

Prediction 2.4: Air temperature displays small but measurable heterogeneity around the transparent glass devices, manifested by a lower temperature below the glass in air volumes directly shadowed by a plate during the day, higher in the air space shielded from direct solar radiation and immediately below the installation height of glass, and highest at elevations above the glass. The relative trend between above- and below-device measurements reverse during the night. The average temperature is higher than underneath mirror devices and amplitude attenuation is also less than under mirror devices. **H_0(2.4) null**: There is no measurable difference in air temperatures at various heights and lateral locations within each clear glass array.

Prediction 2.5: Air temperature is correlated with local cloud cover, wind speed and direction, and antecedent precipitation. **H_0(2.5) null**: There is no measurable correlation between air temperature/humidity and any of the other monitored variables.

Regardless of whether **H_0(1.2)-H_0(1.5)** and **H_0(2.1)-H_0(2.5)** are true or false, environmental parameters obtained through the soil (Section 5.1) and atmosphere (Section 5.2) projects will enable meaningful analysis and interpretation of plant growth rate and physiology in experimental sites that incorporate plant studies (Sections 5.5 and 5.6).

5.3 Snow-Ice longevity

The impacts of mirrors on the environment during the colder half of the year are equally important to understand. Altered energy balance during the winter, as a result of reducing and slowing down visible and infrared radiation fluxes between the ground and the sky can also result in measurable changes with downstream physical and biological consequences. During seasonal cooling, the presence of a layer of glass above the soil-air interface impedes the outward net flux of heat and IR radiation, leading to an expected warming anomaly relative to control. The expected overall impact on the annual cycle may thus mirror diurnal trends, manifested as an attenuation of amplitudes. The impact on values averaged over multiple diurnal cycles needs experimental investigation.

This mirror-cryosphere interaction project is suitable for regions that reliably receive snow precipitation during the winter. It examines the impact of the mirrors on net energy flux at the surface and within snow and ice cover, manifested by changing temperature of the soil, of the snow, and of the air right above it. The altered longevity and melting pattern in micro-environments around the various mirror and glass devices are in addition followed using photos and video recordings. We anticipate several outcomes from the proposed experiments and test these with null hypotheses:

Prediction 3.1: The presence of the mirrors will create a micro-environment under the arrays manifested by cooler snow and soil temperatures during sunny days and a reduction of the diurnal temperature amplitudes. These effects will scale proportionally to the temporal coverage by shadows projected by the mirrors and black glass (Fig. 1). **H_0(3.1) null**: There is no measurable difference in snow and ground temperature, that systematically varies with location of the soil with respect to mirror placement and shadow sweep regions.
Prediction 3.2: Snow and ice will melt at different rates that show spatial correlation with microenvironments around the devices, and that these patterns could be reproducibly document in time series of photos and videos. **H_0(3.2) null**: There is no measurable difference in the rate of snow melting compared to control areas that systematically varies with location with respect to mirror placement and shadow sweep regions.
Prediction 3.3: Compared to mirror devices, snow and ice will melt faster underneath clear glass devices and fastest underneath black glass devices, and that these patterns could be reproducibly document in time series of photos and videos. **H_0(3.3) null**: There is no measurable difference the rate of snow melting underneath the various devices.

5.4 Urban environment

Experiments conducted in urban environments over concrete and asphalt surfaces share much in common with experiments over agricultural and natural soil surfaces. A key difference is the partitioning of surface energy balance terms. Specifically, urban closed surfaces provide little to no water for evaporative cooling, resulting in higher surface temperatures during the day and higher outgoing IR radiation flux. The physical presence of devices compared to an otherwise featureless surface can perturb air circulation, add surface roughness, and increase sensible heat flux. These effects combine to enable the prediction that ground surface temperatures should be reduced in microenvironments around mirror and black glass devices, but that air temperature may not respond in the same way due to potentially enhanced sensible heat transfer from an increase in surface roughness. These effects are likely functions of wind conditions.

5.5 Endemic plant response

This project can be carried out in conjunction with soil moisture studies and assesses the effect of mirror arrays on the growth rate and other physiological measures of the life cycle in plants endemic to the sites. Specifically, we want to examine plant growth, leaf chlorophyll content, and biomass accumulation both above and below ground as a function of mirror coverage. In each mirror array environment, we propose to compare the growth of plants in 4 groups corresponding to the 4 types of micro-environments (Fig. 2). Micro-environmental conditions are measured by sensor networks as described before in the soil and air impact projects. We anticipate several outcomes from the proposed experiments and test these with null hypotheses:
Prediction 5.1: The spatial density of mirrors, and their proximity to each other, has a compound effect

on vegetation growth that changes in a way consistent with plant physiological response to parameters that include temperature, moisture, and solar radiation. $\mathbf{H}_0$**(5.1) null**: Vegetation growth is uncorrelated with microenvironmental conditions around the devices.

If $\mathbf{H}_0$**(5.1)** is false, then

Prediction 5.2: Endemic vegetation growth rate displays heterogeneity within the mirror arrays, and correlates with the micro-environment in which the plants are found (Fig. 2). $\mathbf{H}_0$**(2.2) null**: There is no measurable difference in the growth rate and physiological metrics of the endemic plant in 20 cm x 20 cm sampling areas compared across various micro-environments of an array.

If **H5.2** is false, then

Prediction 5.3: Mirror arrays interact with background climatic conditions to create variability of the growth rate in time. Presence of the mirrors will promote faster growth of endemic species during periods of heat and water stress. During cool periods with abundant precipitation, the presence of mirrors would reduce the growth rates of plants. These effects will be more prominent in plots with larger areal coverage by mirrors (Fig. 1). $\mathbf{H}_0$**(5.3) null**: There is no measurable difference in plant growth rate between representative 20 cm x 20 cm sampling areas within the arrays.

Vegetation growth will be assessed using pre- and post-experiment surveys of existing vegetation within each plot. 3 sampling areas for each micro-environment will be analyzed. The analysis will be repeated monthly throughout the growing season. The exact placement of the sampling areas will be finalized after installation of the arrays, at which point a better assessment of the heterogeneity characteristics can be conducted, including the exact pattern of local shading level and precipitation direction. The sampled vegetation will be identified to species, and measured for overall stem height, root morphology, total wet/dry mass, and the ratio of above- and below-ground biomasses. For some species, it may be possible to compare seed production, numbers and mass of seeds per plant, across the plots.

We foresee that this project requires significant development and repetition over multiple growth seasons due to the complexity of an endemic ecosystem. We will use *in situ* monitoring via field cameras, photography from above the experimental areas, field sampling of leave chlorophyll content, and laboratory analysis of sample biomass to follow plant response. We further foresee the need to expand the sensor network for this preliminary experiment in the future to include measurement of the level and directionality of photosynthetically active light in each of the micro-environments.

In addition to tacking the complexity of an endemic ecosystem of plants, we also propose to study a model plant species for more controllable conditions, as described in Section 5.6.

5.6 Experimental model plant response

We will examine terrestrial plant growth and chlorophyll content of a potted plant, such as *Arabidopsis thaliana*, as a function of mirror coverage. This experiment will mirror the micro-environment design of the endemic plant project (Section 5.5). In each of the 2-by-2 arrays, we will place 20 potted samples, due to 5 micro-environments with 4 replicates each. As much as possible, available sensors will be installed to monitor the micro-environments. These micro-environments are 1) control (south of array), 2) under southern row but not directly shadowed, 3) at the center of the array, in the shadow band of the southern row, 4) to the East of the array, receiving direct morning light and evening shadow, 5) to the west of the array, receiving direct evening light and morning shadow.

Each sample pot will have 7-10 seeds for germination and will be exposed to naturally varying temperatures, sunlight intensity, and photoperiod. Seeds will be sterilized prior to sowing. After sowing and vernalization of seeds we will observe and record details of growth and life cycle stages, timing of germination, percentage of seeds germinated, development of first cotyledon, plant height, leaf area, bolting, flowering, plant weight (gross weight), number of leaves per plant. Seeds will be collected, dried, and stored. After plants are harvested, we will collect data on number of lateral shoots, stem diameter, and plant width, wet/dry weight of stem, leaves, and bracts, area of leaves and bracts, stomata density and length of silique. We anticipate several outcomes from the proposed experiments and test these with null hypotheses:

Prediction 6.1: The various microenvironments generate a measurable effect on *Arabidopsis thaliana* growth that changes in proportion to total shading. $\mathbf{H}_0$**(6.1) null**: Vegetation growth is uncorrelated to microenvironmental parameters such as radiation, soil, and air temperature.

If $\mathbf{H}_0$**(6.1)** is false, then

Prediction 6.2: *Arabidopsis thaliana* growth rate displays heterogeneity within the mirror arrays, and correlates with the micro-environment in which the plants are found (Fig. 2). **H2.2 null**: There is no measurable difference in the growth rate and physiological metrics of *Arabidopsis thaliana* compared across various micro-environments of an array.

If $\mathbf{H}_0$**(6.2)** is false, then

Prediction 6.3: Mirror arrays interact with background climatic conditions to create variability of the growth rate in time. Presence of the mirrors will promote faster growth of *Arabidopsis thaliana* during periods of heat and water stress. During cool periods with abundant precipitation, the presence of mirrors would reduce the growth rates. $\mathbf{H}_0$**(6.3) null**: There is no measurable difference in *Arabidopsis thaliana* growth rate in various micro-environment within the arrays.

To enable this experiments, the pots in which the plants are placed will be customized to enable anchoring to or inserting into the ground so that wind gusts and other weather events would not tip the pots.

5.7 Other possible projects

The system can also be used to investigate many other adaptation-relevant processes. We list a few more examples here. The evaporation of water can be studied by placing a dense array of beakers, carefully weighed before and after the addition of a precise amount of water, to cover the microenvironments around the mirror device and array. It is important to note that the choice of the color of the container in this experiment is likely to significantly impact the outcome of the experiment. The impact on marine ecosystems can start to be investigated by placing a similar array but identically inoculated with a strain of algae. This experiment should be conducted using transparent containers.

5.8 Data collection

In addition to the ground-level sensors, each site will be continuously monitored for ambient atmospheric conditions, including air temperature, relative humidity, incoming visible light, and wind speed. While these factors are unlikely to vary significantly within each site, the data about them will help in interpretation of the ground sensors and plant growth measurements. For example, if the entire month of June ends up being unusually cloudy, wet and cool, then differences created by the presence of mirrors may be minimal compared to differences in a predominantly clear, warm and dry month. As a result, data collection will be continuous through a minimum of 3 months. And efforts should be made to ensure continuous data collection over at least 2 years, careful written and photographic documentation of major weather events including, but not limited to, snow, melting, hurricanes, hail, drought, heatwaves, and flooding.

5.9 Resource and data sharing

Sharing of resources, experimental findings and lessons learned across the disciplines are interwoven STEM education outcomes for this project, and are fundamentally based in principles of open education in the pursuit of global solutions to the climate dilemma. Partners working together to facilitate this work through the MEER Framework include all the participating citizen scientists, university and school instructors, and university PIs currently directing large field experiments. Additional partners are students at all these institutions, including participants in PI Doner's NSF-funded GeoPathways project, students in courses Tracy Lesser at NHTI mentors, students and volunteers from affiliated with MEER, and the kindergarten, primary school, and secondary school instructors who incorporate visits to the field site, and/or utilize the demonstration kits in their lessons.

6 Devices, geometric structure, and array design

To eliminate device design and geometric variations as an uncontrolled parameter, participating sites in the global network all use the same standard set of mirror and glass devices, as well as a shared set of sensors. We encourage different sites to acquire additional sensors such as field cameras, infrared imaging devices, vector wind sensors, and soil moisture probes, to achieve more comprehensive coverage and sampling of environmental parameters.

6.1 Package content

The kit contains 6x each of mirrors, black glass, and transparent glass for a total of 18x devices in the kit. 18x machined cedar wood adaptors, complete with a plastic interface for double-sided suction cups, are also included (5x suction cups per device). 20x 1-meter-long glass rod stands are provided for the devices, including one for the custom weather station and one extra for anchoring some sensors and as a replacement in case of breakage at one of the devices due to mishandling or other processes.

6.2 Device geometry and structure

The mirrors are 60 cm square thin reflective films stabilized by an underlying glass plate. The overall thickness is 6 mm, of which 2 mm is the glass mirror, about 1 mm is glue adhesive holding the mirror to the supporting glass, consisting of a 3 mm layer of tempered glass. The black and transparent glass are also 60 cm squares of 4 mm thickness. Each device will be mounted so that the center point of the plate is 50 cm off the ground. The plane of the horizontal device should also be 50 cm above the ground. The devices will be tilted 20° from horizontal during the summer and 45° from horizontal during the winter. These angles are prepared and cut into the wooden adaptor blocks supplied with the kit. This combination of angles were chosen by analyzing the coordinates of the participating site locations, so as to ensure both good average local cooling (maximal frontal exposure to the sun at solar noon) and global cooling (maximal rejection of solar radiation power through atmosphere). Solar elevation for each site was obtained using (suncalc.org). A description of the partitioning of the 18 devices into small sub fields is as follows:

6.3 Device allocation to experimental plots

- Control plot, 0% shade, no devices
- 2×2 mirror array, 4 mirrors
- 2×2 black glass array, 4 black glass plates
- 2×2 transparent glass array, 4 transparent glass plates

- horizontal mirror, permanent installation, 1 mirror
- horizontal black glass, permanent installation, 1 black glass plates
- horizontal transparent glass, permanent installation, 1 transparent glass plates
- horizontal mirror, post-snowfall installation, 1 mirror
- horizontal black glass, post-snowfall installation, 1 black glass plates
- horizontal transparent glass, post-snowfall installation, 1 transparent glass plates

The "post-snowfall" devices is available for various uses in customized experiments in studies that do not involve snowfall. For example, one may juxtapose both horizontal devices side by side to create shadowed regions with higher effective direct shadowing. One could also use both devices to create duplicated, identical measurements. One could also use them to study impact on different surfaces and structures underneath identical shading conditions, such as the growths of two cultivars of lettuce, the evaporation from bins of soil, or from bins of water, etc. The possibilities are numerous.

7 Installation Procedure

7.1 Unpacking

Mirrors and all other supplies will arrive in large cardboard boxes. Glass parts are fragile. Please make sure there is enough space to work safely, for you and the equipment. Place padding material on the ground to receive the glass rods and the glass plates. Open the box and carefully remove all materials leaving the plywood box holding the mirrors. Once everything else is removed, unscrew top and side pieces from the plywood box to access the glass sheets. Once top and sides are removed carefully remove the glass sheets and place on a flat surface away from potentially falling objects from above, that would break the glass. Mirror devices need to be sealed at the edges by a mirror sealant before deployment. MEER team will try to complete this step before packaging and shipping. Please examine the edges and contact MEER if the sealant is not visible.

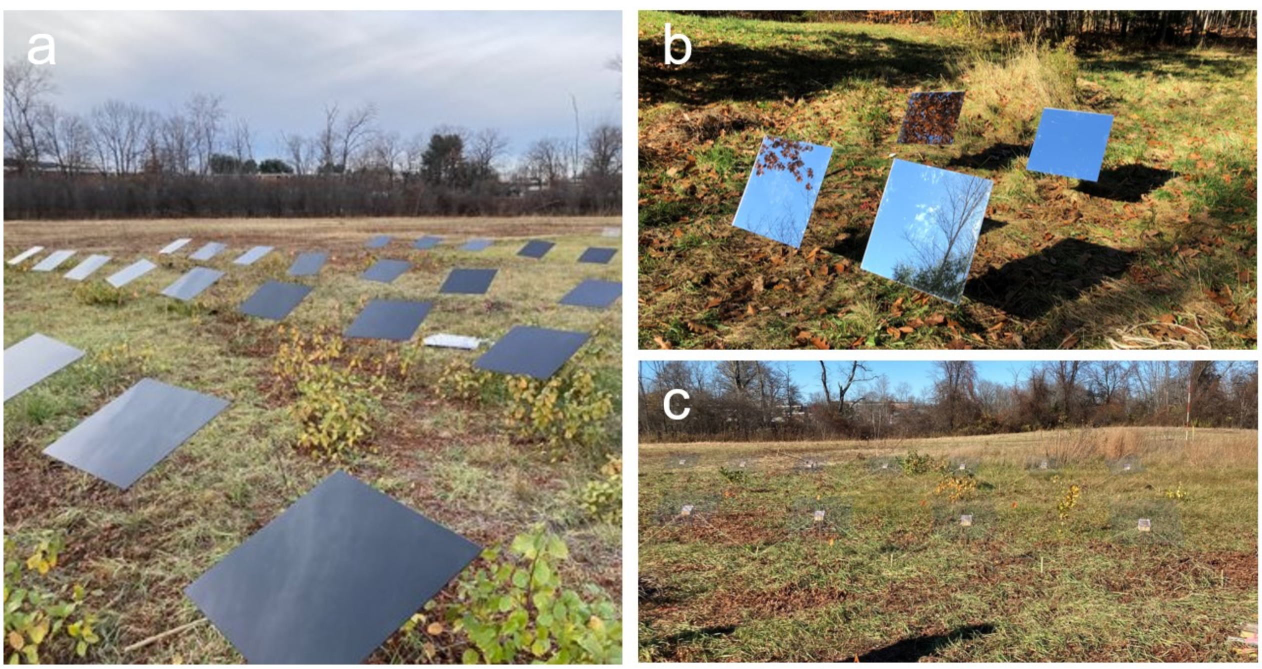

Figure 1: Examples of glass and mirror device arrays used in the experiments (photo credit: Tracey Lesser and Peter Maslan). (**a**) An array of black glass devices (22° tilt) photographed on a cloudy autumn day. (**b**) A 2-by-2 microarray of mirror devices (45° tilt) on a sunny autumn day. (**c**) An array of clear glass devices (22° tilt) photographed on a sunny autumn day. Notice the lack of clearly-visible shadows from the glass, as observed for mirror devices under sunny conditions in **b** and from other objects in **c**.

7.2 Experimental site selection

Several factors need to be weighed in choosing an optimal experimental field. The decision is a balance among several potentially conflicting considerations 1) physical uniformity of the site to minimize uncontrolled topographical and other environmental variables, 2) safety for the experimental equipment and data loggers, 3) lack of human and animal disturbance, 4) possibility of access by the experimental team and by citizens and school classes at a later date for educational and media outreach purposes.

7.2.1 Topographic requirement

The experimental site should be as flat as possible, with a background soil and vegetation that is as uniform as possible. Good examples of site selection are in Fig. 1**a** and Fig. 1**c**. No major intrusion by shadow from nearby structures and tall vegetation throughout the annual solar cycle. A bad example is in Fig. 1**b**. When assigning different parts of the chosen plot to different devices and configurations, there cannot be

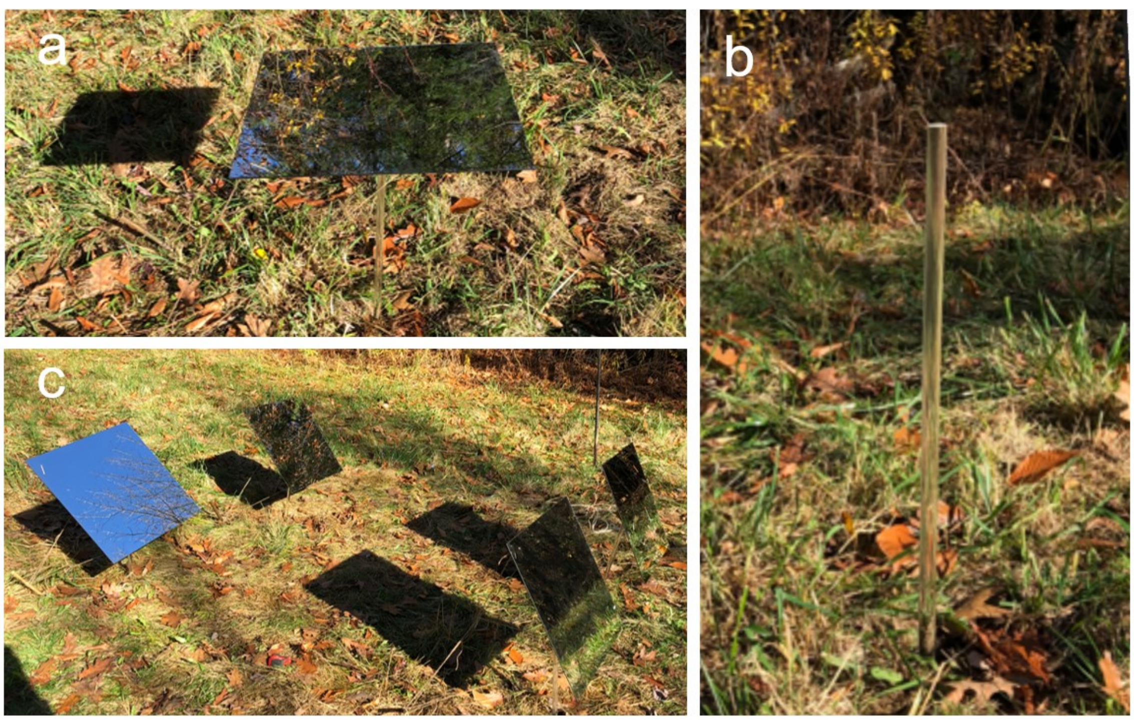

Figure 2: The 3 experimental configurations for each device type (photo credit: Peter Maslan). (**a**) A horizontal device installed on a permanent basis for the duration of the experiment. Snowfall would lead to the accumulation of snow above the device. Vertical distance between the soil and the glass plate is 50 cm. (**b**) A glass rod is prepared and ready to receive a plate-wooden adaptor assembly, after uniform accumulation of ground snow. The device configuration after the assembly would be identical to that in **a**. Snow on the other hand, would be below the plate, rather than above it. (**c**) A 2-by-2 microarray of mirrors prepared in the Winter configuration (45° tilt). The centers of the mirrors are 50 cm above the soil-air interface.

visible differences for areas devoted to mirrors, black glass, and clear glass devices, or among the 3 geometric configurations for each plate material (Fig. 2).

7.2.2 Safety requirement

Due to an angled, sun-facing design, devices in the Northern Hemisphere are more sensitive to northerly wind, and vise-versa for those in the Southern Hemisphere. Wind from direction of the poles creates a lift force. The force due to wind with a horizontal speed of 33 m per second, or 120 km per hour, on a 45° is about 160 Newtons. If this force is distributed over 2 attachment points on the mirror surface, due to installation imperfection and wobbling, each chord would need to handle about 100 Newtons. A 1/32 inch stainless cordage is about sufficient to handle these loads, though a 1/16 inch OD material is preferable. In addition to tie-down with a proper selection of the mirror interface part (Fig. 4), cordage material (Fig. 5), and cordage-ground anchor (Fig. 5), it is also advisable to seek sites that are protected by trees and other tall structures on the side facing the pole. In the absence of such structures, participants should work towards installing a robust 2-m tall windbreak fence 3 meters North (South) of the experimental installation in the Northern (Southern) hemisphere.

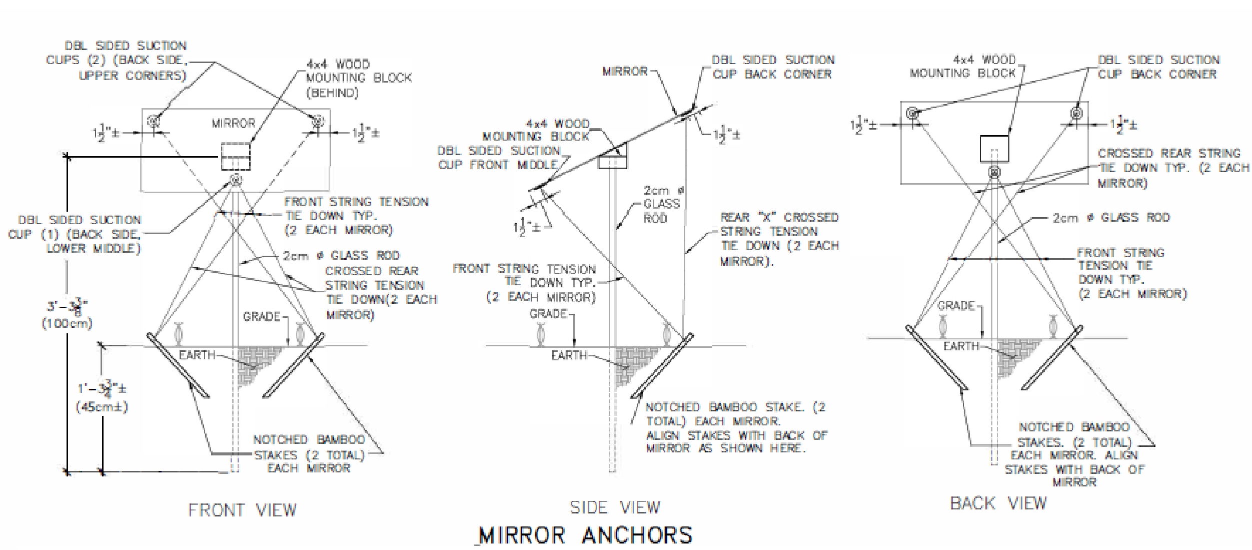

Figure 3: An example of tie-down design for illustrative purposes only. The actual deployment requires a more robust configuration involving tie-down forces applied downwards from the frontal side of the glass plate. More appropriate parts are illustrated in Fig. 4 and Fig. 5.

Fig. 3 provides the general idea for performing a tie-down from the plate directly to the ground. The tie-down is essential for two purposes, constraining rotation of the plate, and preventing liftoff of the plate due to wind. The actual process requires more robust materials compared to what is illustrated and provided in the kit. In particular, all three components that go into the tie-down need to be of high quality. The 3 parts are padded

Figure 4: Examples of glass clamps to enable safety tie-down of glass plates. The thickness of glass used with these commercially available clamps are generally thicker than the devices for the experiment. The mismatch can be resolved by placing a 3mm-thick piece of plastic shim, about 1-by-1 inch or slightly larger, that both leads to good thickness fit and also distribute the point force over a larger area. The color of the plastic should be made to match that of the mirror and glass devices.

metal clamp to interface with the glass plate, stainless steel cable for providing tension, and a ground anchor screw. Examples of acceptable parts are provided in Fig. 4 and Fig. 5. These parts need to be purchased by the participants and are absolutely necessary to ensure the success of the experiments over hopefully many years of experimentation.

7.2.3 Access control

Each site should strive to minimize uncontrolled access by people, pets, and large wildlife. This can be achieved by a combination of physical barriers and information signage describing the nature and importance of the ongoing experiments. The signages should be installed on the polar side of the field experiment, to serve the dual purpose of a wind break, and to avoid creating sources of shadows that impact the experiment. All participant will collaborate to write the content for these signage and design the graphics. We should aim to have several different panels, each for a different type of glass or mirror, and also panels that give more upper-level overview of the MEER concept and also an overview of the various experiments going on within MEER-iREC.

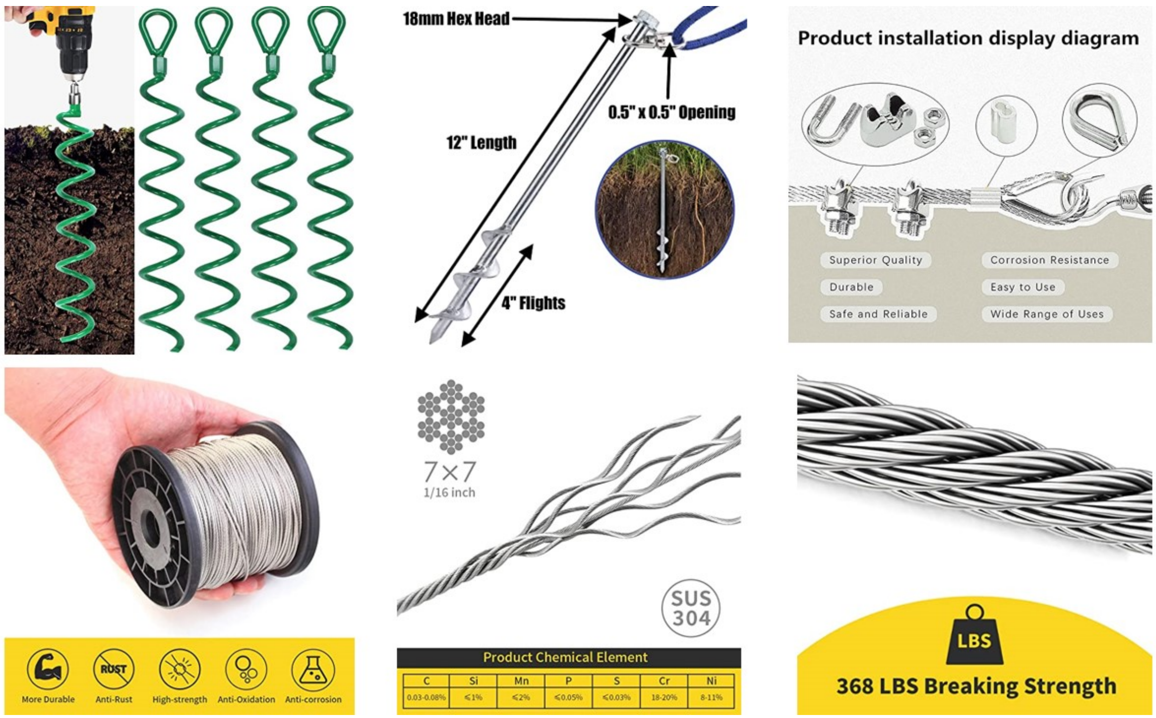

Figure 5: Examples of ground anchor and stainless steel cable for tie-down. We suggest 1/16 inch (1.5 mm outer diameter) stainless steel cables for the tie-down. a minimum gauge of 1/32 inch is necessary for the expected loads. Commercially available parts for cable handling and adjustments are also illustrated.

Design and execution of the appropriate fencing mechanism is another technical area where participants should collaborate on. An relatively easy approach is to use the same stainless steel cordage in tie-down as the basis for constructing the fencing. Alternative ideas and specific details are to be worked out in group meetings.

7.3 Experimental site preparation

After site selection and partitioning into plots for the various devices and arrays, installation can be done a number of ways, depending on the nature of the ground. One that may prove highly efficient for soil is to drive a steel stake around 20 mm in diameter into the ground where you want a glass pole to stand. A major challenge is to create a hole that points perfectly downwards, so the resulting devices look both visually perfect, and also project shadows exactly as designed based on solar path analyses. Another challenge has a chance element about it; there are occasionally rocks in the ground, running into one might mean requiring to parallelly shift an entire array.

7.3.1 Planning for the seasons

Both the length and the positions of shadows projected by mirrors and glass vary as a function of both the season and the chosen device tilt angle. One should therefore prepare multiple device implantation/arrangement geometries in one go, to avoid the future need to repeat this procedure. There needs to be multiple sets of holes pre-drilled for the 2-by-2 array. At least two sets are necessary, for the summer and winter halves of the year. One could also envision 3 sets of holes, with one set for spring and fall, or an even finer division, based on the specific needs of the experiment. The different sets of holes could share the same southern pair of holes. In that case, the northern pair should be progressively farther away from the souther pair as time moves from summer to winter. It is important that the wind break be placed farther than the reach of the shadow of the Northern devices, for that shadow region is part of experimental investigation.

The exact measurements for each of the seasons need to be customized on a case-by-case basis, as a function not only of the latitude of the experimental site, but also of the specific planned experiment, which includes consideration, for example, of the footprint of pots and beakers for experiments that investigate plant growth and water evaporation, respectively. Individual sites need to individually work with Dr. Tao to determine these site-specific parameters.

7.3.2 The perfect array

To make perfectly rectangular arrays, guide strings are useful. Tie a string that is longer than the size of the array (example: if 4 columns or rows of devices are to be implanted with 100 cm between each in the East-West orientation, cut a string approximately 450 cm in length.) to a stake inserted at a first chosen corner of the array. Pull this string out in one of the cardinal directions towards the other corner (Fig. 6e): North, South, East, or West (depending on which corner you started with). Once you have pulled the string taut and fixed it by placing some weight over it, measure the required inter-column or inter-row distance. Mark the location of the point with a visible stick. For large arrays, there would be many rows or columns marked. For this citizen science experiment, we are only dealing with 2 devices in each direction.

Repeat this process for the other orthogonal direction using another string, making sure the two strings indeed make 90 degrees. Consider using a large object with a known 90 degree angle. From there, locate the 4th corner, and make sure that the two diagonals are of equal lengths before moving on to drill the holes to depth.

The distance between each device in the N-S orientation will be different for each site as a result of solar elevation at noon, and varies depending on the season of experiment and purpose of the experiment. The choice of inter-row separation will be discussed and calculated on a case-by-case basis. We use, however, a standard, inter-column (E-W) separation of 1 meter for these experiments.

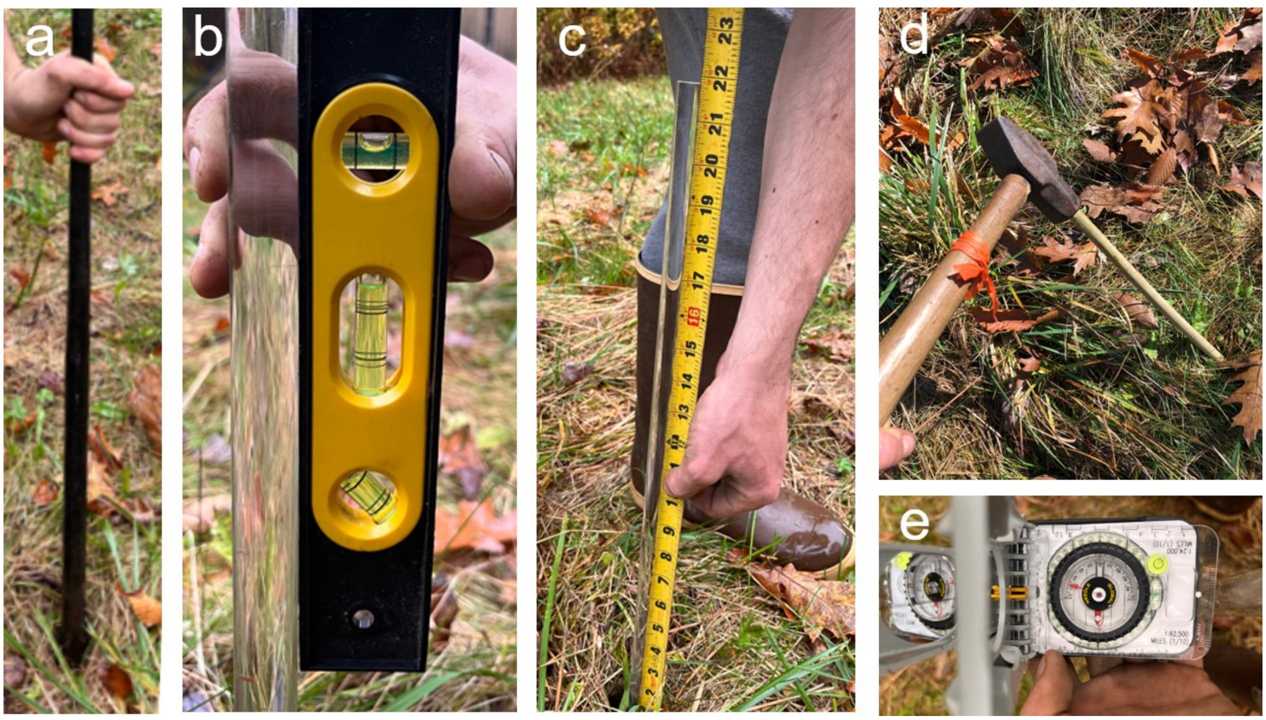

Figure 6: Techniques for perfect array geometry. (**a**) A metal stake is used for pre-drilling holes for planting the glass rods. Letting gravity act on the center of the gravity of the stake ensures verticality. (**b**) A level is essential for checking verticality both during pre-drilling with the stake and upon installation of the glass rod. The measurement needs to be performed from both orthogonal direction. (**c**) The implantation depths (different from that illustrated) need to be precisely controlled. The goal is to achieve 50 cm distance between the air-soil interface and the center of the plate. (**d**) When using a smooth, featureless rod for tie-down, the anchoring stakes need to be inserted into the soil at an angle such that it makes a angle less than 90° with the tension cordage. This is to ensure that no slipping off from the tip could happen. (**e**) A compass that provides geographic North (instead of magnetic North) is necessary for both establishing the orientation individual devices, and for planning out perfect rectangular arrays precisely oriented parallel and orthogonal to the cardinal directions.

7.3.3 Making straight vertical implantation holes

A trick for achieving a straight hole is to hold the top of the steel stake such that it hangs motionless, pointing down as one slowly lowers it to touch the soil surface at the design location (Fig. 6a). Start driving it into the ground with a hammer without laterally moving the upper tip. It may be useful to have two other people to help looking from orthogonal directions during this procedure. Continue driving until the insertion start to constrains rotation. Check the verticality of the stake using a level (e.g., see Fig. 6b). Try correcting small imperfections and re-measure periodically. For concrete and asphalt surfaces, it is advisable to build a jig that guides the initial drilling until verticality is established. It takes practice to achieve perfectly straight holes. Participants should practice this procedure over unimportant locations before doing it over optimally chosen experimental plot locations.

For angled and horizontal devices alike, the final height at the center of the devices should be 50 cm above the air-soil interface. We suggest first drill a hole that is 50 cm deep, make a test assembly run, measure the actual height of the center point, and then adjust the depth of the hole accordingly.

7.4 Expectation for participants for durability, safety, and controlled access

Durability of the infrastructure and its safety for the surrounding area is key. For this reason, all participating sites need to 1) adhere to the current best practice in device installation, 2) actively contribute to improving the engineering robustness and security of the device tie down method, 3) Set up the necessary wind breaks and perimeter markers to prevent and minimize intrusion by pedestrians, dogs, and other animals, 4) collaboratively develop outdoor, information signs to be erected at the sites to educate passerby about climate change science, ecology, and MEER adaptation experiments, as well as to discourage unauthorized and undocumented access to the vicinity of the experimental site, which could lead to both falsification of data and damage to infrastructure.

As stated before, experimental site should be chosen such that no shadow passes through it throughout the year. Due to the sun-facing angled design of the devices, the devices in the Northern Hemisphere are more sensitive to northerly wind, and vise-versa for the Southern Hemisphere, which creates a lift force. It is thus advised to seek sites that are protected by trees and other tall structures on the side facing the pole. In the absence of such structures, we advice the participants to install a windbreak fence 3 meters to the North (South) of the experimental installation.

Once properly completed, instrumented, and wind-protected using, for example, informational signage, the test location can offers opportunities for both unsolicited outreach and informal education, as well as formal education associated with courses and outdoor labs during school sessions.

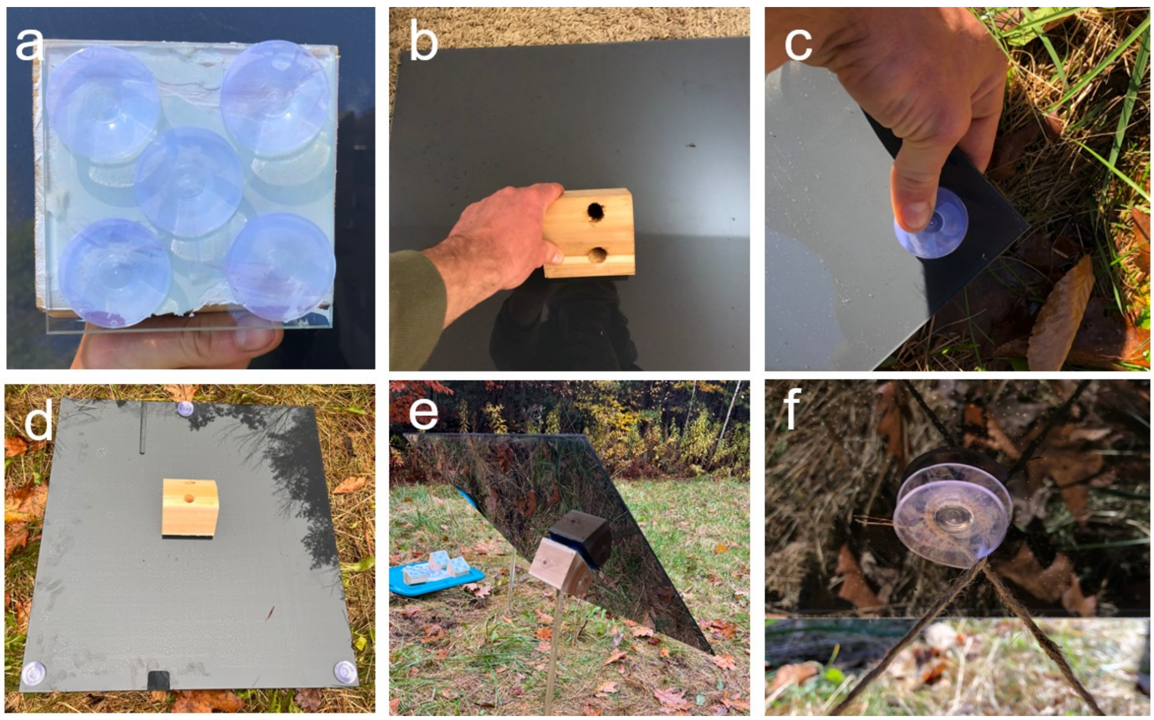

Figure 7: Sequence of steps for a safe assembly of devices. (**a**) Double-sided suction cups are carefully cleaned with alcohol wipes and fixed onto an equally cleaned, optically smooth surface (either glass or acrylic) affixed onto the top of the angled wooden adaptor. (**b**) The attachment of the wooden block to the glass plate can take place **only when** the glass rests securely supported on a **completely flat** surface, such as a clean, wooden bench top. Otherwise, the downward pressure at the center would crack and break the glass through torque generation. **The carpet floor in the picture is far from optimal and should not be used** (**c**) Attach the tie-down mechanism onto the glass plate. Illustrated here are double-sided suction cups, which should not be used for this purpose. The better part to use are those in Fig.4. (**d**) A view of the glass-wooden adaptor assembly before attachment to the glass rod. (**e**) The plate-wooden adaptor assembly is gently positioned over the pre-prepared glass rod in the ground. The assembly should be manipulated by holding directly onto the wooden block. (**f**) Tie-down cordage is attached from the angled ground anchor to the tie-down attachment points on the glass. Adjust until there is tension established in the cords. Stronger stainless steel based cordage should be used in practice. The twine and suction cups are shown only for illustrative purposes. The proper system to use are from parts shown in Fig.4 and Fig.5.

8 Sensor Placement

Weather Station: Each site is supplied with a custom weather station that logs air temperature, air humidity, and monitors downwelling solar radiation and wind speed. The sensing is based on Elitech's temperature and humidity sensor RC-4HC. Radiation shielding is achieved using mirrored plastic boards. Photon sensitivity is achieved using solar paint, and wind sensitivity is achieved by differential comparison between wind-shielded and wind-exposed probes. A total of 3 RC-4HC loggers are used in the Weather Station

Ground temperature: Each site is equipped with 18 soil temperature probes based on Elitech's RC-5+. Each probe is inserted into the soil surface at a depth of 2 cm.

Ground interface: Each site is equipped with 18 radiation-shielded, soil-air, soil-snow interface sensor based on Elitech's RC-5+.

Glass temperature: Each site is equipped with 3 sensors that measure the temperature of the glass surface on the underside. They are based on Elitech's RC-HC4. The devices also measure the humidity directly underneath the plates.

Air temperature: Each site is equipped with 13 radiation-shielded air temperature and humidity sensor based on Elitech's RC-4HC. 1 is used as control. 4 are dedicated to each device type, of which 3 are installed

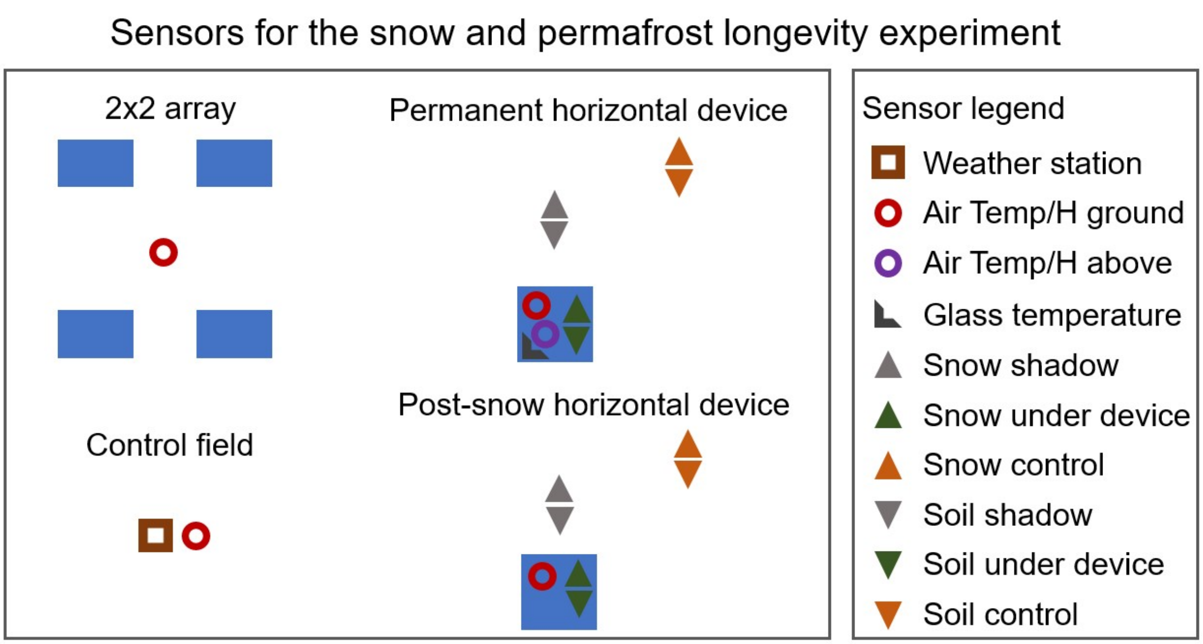

Figure 8: Approximate sensor placement for mirror-snow and mirror-cryosphere interaction projects. Instrumentation for one of three device types is provided.

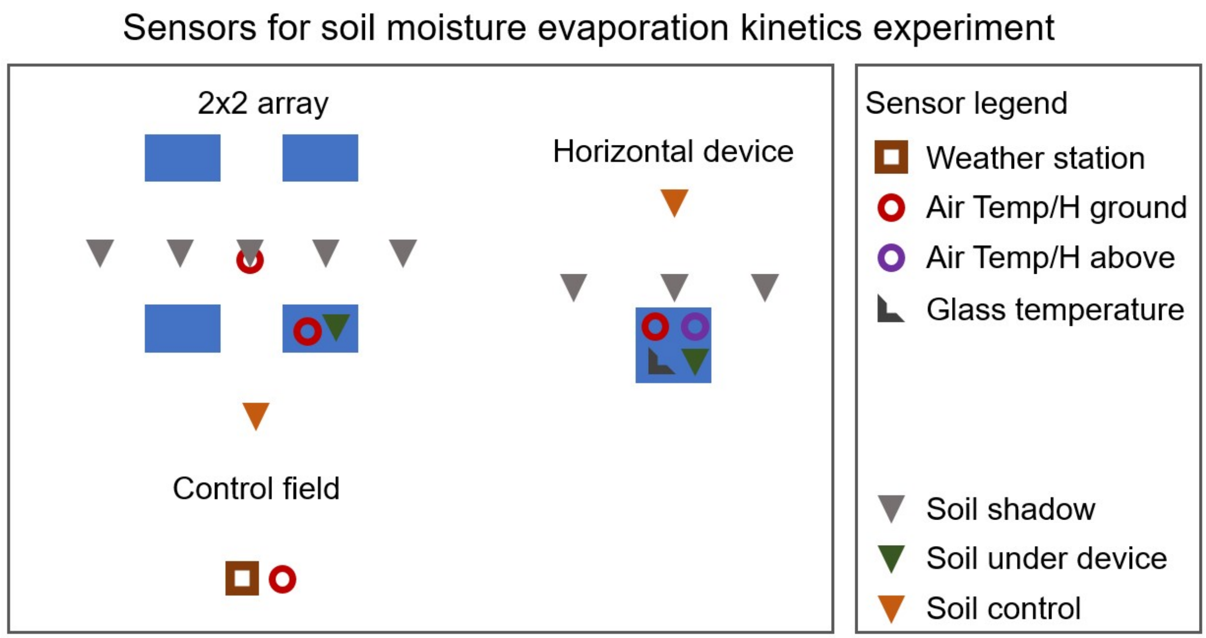

Figure 9: Approximate sensor placement summer soil moisture projects. Instrumentation for one of three device types is provided.

underneath each of the 3 configurations, and 1 is installed above the horizontal device.

The total number of data loggers is 55 and detailed in Tables in Section 12.

9 Specific aims

9.1 Temperature trends as a function of micro-environment

The experimental design is set up to allow determination of spatial trends in temperature across the spring and summer growing seasons, as well as snowy winter seasons, under different sized shade versus sunlit areas, below and above ground. It tests the primary null hypothesis : there is no measurable difference in ground temperature between the control plot and any of the plots with glass devices.

9.2 Moisture content trends as a function of micro-environment

The experimental design is set up to allow determination of spatial trends in soil moisture and air humidity across the spring, summer, and fall seasons, and under different types of shade versus sunlit areas. As with the temperature data, it tests the primary null hypothesis : there is no measurable difference in soil moisture between the control plot and any of the microenvironments in plots with glass devices. Confounding factors for soil moisture are local water table variations and channeling of rain off the mirror surfaces. These are not controlled for in the experimental design but can be assessed from atmospheric sensor data retrieved at the plot sites.

9.3 Intra-plot spatial heterogeneity

Heterogeneity within each plot includes intrinsic variability of the soil and ground in the lateral dimensions. Random error induced by variable sensor burial depth also contribute. These influences will be controlled and analyzed by taking time series with sensors in place in the absence of glass and mirror devices. The resulting time series serve as background data. Ground variations will influence the exact extent of shading; these will be minimized as a much as possible selecting level ground within the plot for each device type, ideally completely level for all 3 device types. Another technique to tease out random variability from specific impact of the devices is to rotate the 3 types of devices around, by detaching at the glass rod-wooden block junction. We propose the following frequency and timing of measurements:

- from the ground-level air temperature and buried soil temperature sensors,, at 10 minute intervals over a 21-day interval prior to device placement,
- Air temperature and moisture sensors: 5 minute intervals over the entire experimental period
- Shortwave radiations and wind speed: 1 minute intervals over the entire experimental period

9.4 Primary production trends as a function of mirror coverage

The experimental design is set up to allow determination of spatial trends in the response of primary production across the spring and summer growing seasons, under different sized shade versus sunlit areas. It tests the primary null hypothesis : there is no measurable difference in primary productivity between the control plot and any of the plots with mirror arrays.

9.5 Primary production trends as a function of intra-plot micro-environment

The experimental design is set up to allow determination o trends in the response of primary production across the spring and summer growing seasons, within different characteristic microenvironment arising from the discrete nature of individual mirrors in an array. It tests the primary null hypothesis : there is no measurable difference in primary productivity among samples grown in different micro-environments.

9.6 Maintenance of the field arrays and anticipated problems

There are a number of uncontrollable factors that may disrupt the experiment, but the most likely are vandalism, damage caused by animals (especially to data cables), severe weather (hail), dust storms, hurricanes, flooding of field areas with soil saturation lasting more than 24 hours, and sensor battery drainage and sensor corrosion causing data loss. Regular battery replacement will be conducted to minimize data loss from electrical outages. And data will be downloaded every two weeks and backed up on multiple local and cloud storage locations. One Daily visits to the array will include checks for damage, and repair as needed. Deer fencing will be installed to reduce the likelihood of larger animal incursions. Information signage will be erected for educational outreach and to minize pedestrian ingress and disturbance.

Site visits by educational groups will keep visitors outside the perimeter of the whole array, with a demonstration model available to show the arrangement of the sensors. Live data feeds will be accessible via an outward facing weblink. Only approved researchers will have access to the raw data.

10 Data Management Plan

Access to all the data will be available for download within 1 years of the end of the experiment. Selected excerpts will be available for educational uses during the experiment. All the data will be centrally stored by MEER and made available for download through MEER.org for research and educational purposes.
With future funding, we will establish internship positions dedicated to developing accessible summaries of the data and other educational materials in the forms of digital flyers, YouTube channel videos, QUBES content, and social media posts to inform the public stakeholder of the day-to-day achievements of our teams and the latest experimental findings.

11 Open education and public engagement goals

We are committed to open science education, research, and collaboration. Our goal is to demonstrate the feasibility of collaborating with educators and students in k-12 and higher education, as well as the global public who are all stakeholders in this project.

11.1 In higher education

We are committed to involving undergraduate and graduate students in MEER-iREC research. Each site is committed to reach out to local universities to inform their ecological, agricultural, and engineering departments of the experimental sites. Intern applicants from universities and neighbor schools will be selected to participate in the research to gain experience in the process of science and collaboration through helping to design, set up, measure, collect daily data, assist with maintenance of the arrays, analyze data and communicate findings with members of this team, as well as develop outreach materials for social media sites and the project website. Both remote and on-site positions will be made available. Also, much of the work we conduct will be transferable to higher education classrooms so that future experiments can be conducted in the classroom to provide greater insight into the effects of passive adaptation technologies and an opportunity for students to participate in an innovative science project.

11.2 At pre-university levels

We are committed to working towards developing feasible protocols and materials so that these experiments can be conducted in upper elementary, middle school, or high school classrooms. The nature of this multidisciplinary experiment gives it the potential to be integrated into the science curriculum and align with many of the science standards and aspirations in the third decade of the 21st century. For example, science standards in the state of New Hampshire refer to plant growth, photosynthesis, the science process, and human impacts on the environment which directly connect to this experiment. There are also opportunities to connect the engineering design process to science experiments as students can help to improve on the experimental design and set up. Lastly, the general design and size of demonstration kits makes it possible to reach more distant schools and students and expanding to more rural parts of our state. Our goal is to work to develop a feasible protocol, materials, and the connection to standards for interested educators in hopes of potentially creating a small network among schools across the globe.

11.3 For the public stakeholder

Qualified volunteers would also be allowed to participate in and contribute to experimental implementation and data analysis, on a case-by-case basis as determined and approved by the principal investigators supervising the project.

11.4 The Student Colleague Model

As much as possible, students and citizen scientist volunteers will be treated as research colleagues and encouraged to perform the work as part of an internship or undergraduate research project, with mentoring by PIs and the MEER project team. This mentoring commitment includes training in specific tasks, problem solving, communication training, mentoring by example, and guidance in leveraging the experience and network connections for further advancement. Project ownership will be encouraged to develop self efficacy and confidence as researchers.

12 Sensor List

This section provides lists of sensor deployment for the snow longevity and soil moisture projects. Sensor configuration for other studies are similar, with decisions that can be customized based on experimental needs.

SENSOR NAME	ABBREV.	LOGGER[a]	COUNT	CONTROL	MIRROR	BLACK	CLEAR	**# LOGGER**
Weather Station	WS	RC-4HC	3	1				3
Air Above	AA	RC-4HC	1		1	1	1	3
Air Below	AB	RC-4HC	1		3	3	3	9
Air control	AC	RC-4HC	1	1				1
Glass Temp	GT	RC-4HC	1		1	1	1	3
Soil Shadow	SS	RC-5+	1		2	2	2	6
Soil Under	SU	RC-5+	1		2	2	2	6
Soil Control	SC	RC-5+	1		2	2	2	6
Ice Shadow	IS	RC-5+	1		2	2	2	6
Ice Under	IU	RC-5+	1		2	2	2	6
Ice Control	IC	RC-5+	1		2	2	2	6
TOTAL[a]								55

Table 1: Snow longevity-sensor names, placement, and logger count [a] This is the number of logger in each instrument. [b] This is the total number of logger deployed at a site.

SENSOR NAME	ABBREV.	LOGGER[a]	COUNT	CONTROL	MIRROR	BLACK	CLEAR	**# LOGGER**
Weather Station	WS	RC-4HC	3	1				3
Air Above	AA	RC-4HC	1		1	1	1	3
Air Below	AB	RC-4HC	1		3	3	3	9
Air control	AC	RC-4HC	1	1				1
Glass Temp	GT	RC-4HC	1		1	1	1	3
Soil Array	SA	RC-5+	1		5	5	5	15
Soil Shadow	SS	RC-5+	1		3	3	3	9
Soil Under	SU	RC-5+	1		2	2	2	6
Soil Control	SC	RC-5+	1		2	2	2	6
TOTAL[a]								55

Table 2: Soil moisture-sensor names, placement, and logger count [a] This is the number of logger in each instrument. [b] This is the total number of logger deployed at a site.

References

[1] Trisos, C. H., Merow, C., and Pigot, A. L. *Nature* **580**, 496–501 (2020).

[2] Hsiang, S. M., Burke, M., and Miguel, E. *Science* **341**, 1235367 (2013).

[3] Institute, W. R. Accessed February 28th (2021).

[4] Stults, M. and Woodruff, S. C. *Mitig. Adapt. Strateg. Glob. Chang.* **22**, 1249–1279 (2017).

[5] Olazabal, M., Galarraga, I., Ford, J., Murieta, E. S. D., and Lesnikowski, A. *Int. J. Urban Sust. Dev.* **11**, 277–296 (2019).

[6] Kang, S. and Eltahir, E. A. *Nat. Commun.* **9:2894** (2018).

[7] Frölicher, T. L., Fischer, E. M., and Gruber, N. *Nature* **560**, 360–364 (2018).

[8] Sailor, D. J., Baniassadi, A., O'Lenick, C. R., and Wilhelmi, O. V. *Environ. Res. Lett.* **14**, 054006 (2019).

[9] Lobell, D. B., Schlenker, W., and Costa-Roberts, J. *Science* **333**, 616–620 (2011).

[10] Wheeler, T. and von Braun, J. *Science* **341**, 508–513 (2013).

[11] Ehrlich, P. R. and Harte, J. *PNAS* **112**, 14743–14744 (2015).

[12] Zampieri, M., Ceglar, A., Dentener, F., Dosio, A., Naumann, G., van den Berg, M., and Toreti, A. *Earth's Future* **7**, 113–122 (2019).

[13] Ray, D. K., West, P. C., Clark, M., Gerber, J. S., Prishchepov, A. V., and Chatterjee, S. *PloS ONE* **14**, e0217148 (2019).

[14] Hatfield, J. L., Reginato, R. J., and Idso, S. B. *Agric. For. Meteorol.* **32**, 41–53 (1984).

[15] Choudhury, B. J., Idso, S. B., and Reginato, R. J. *Agric. For. Meteorol.* **39**, 283–297 (1987).

[16] Gowda, P. H., Chavez, J. L., Colaizzi, P. D., Evett, S. R., Howell, T. A., and Tolk, J. A. *Irrig. Sci.* **26**, 223–237 (2008).

[17] Ştefan Dezsi, Mîndrescu, M., Petrea, D., Rai, P. K., Hamann, A., and Nistor, M. *Int. J. Climatol.* **38**, 3823–3841 (2018).

[18] Thorp, K. R., Thompson, A. L., Harders, S. J., French, A. N., , and Ward, R. W. *Remote Sens.* **10**, 1682 (2018).

[19] Li, X., Peng, S., Xi, Y., Woolway, R. I., and Liu, G. *Nat. Commun.* **21**, 13:5156 (2015).

[20] Huang, L., Timmermann, A., Lee, S.-S., Rodgers, K. B., Yamaguchi, R., and Chung, E.-S. *Nat. Commun.* **13**, 5798 (2022).

[21] Shaffer, C. D., Alvarez, C., Bailey, C., Barnard, D., Bhalla, S., Chandrasekaran, C., Chandrasekaran, V., Chung, H.-M., Dorer, D. R., Du, C., Eckdahl, T. T., Poet, J. L., Frohlich, D., Anya L. Goodman, Y. G., Hauser, C., Hoopes, L. L., Johnson, D., Jones, C. J., Kaehler, M., Kokan, N., Kopp, O. R., Kuleck, G. A., McNeil, G., Moss, R., Myka, J. L., Nagengast, A., Morris, R., Overvoorde, P. J., Shoop, E., Parrish, S., Reed, K., Regisford, E. G., Revie, D., Rosenwald, A. G., Saville, K., Schroeder, S., Shaw, M., Skuse, G., Smith, C., Smith, M., Spana, E. P., Spratt, M., Stamm, J., Thompson, J. S., Wawersik, M., Wilson, B. A., Youngblom, J., Leung, W., Buhler, J., Mardis, E. R., Lopatto, D., , and Elgin, S. C. *CBE Life Sci. Educ.* **9**, 55–69 (2010).

[22] Caruso, J. P., Israel, N., Rowland, K., Lovelace, M. J., , and Saunders, M. J. *J. Microbiol. Biol. Educ.* **17**, 156–162 (2016).

[23] Hanauer, D. I., Graham, M. J., SEA-PHAGES, Betancur, L., Bobrownicki, A., Cresawn, S. G., Rebecca A. Garlena and, D. J.-S., Kaufmann, N., Pope, W. H., Russell, D. A., Jr., W. R. J., Sivanathan, V., Asai, D. J., , and Hatfull, G. F. *PNAS* **114**, 13531–13536 (2017).

[24] Trenberth, K. E. *J. R. Soc. N. Z.* **50**, 331–347 (2020).

[25] Hansen, J., Nazarenko, L., Ruedy, R., Sato, M., Willis, J., Del Genio, A., Koch, D., Lacis, A., Lo, K., Menon, S., Novakov, T., Perlwitz, J., Russell, G., Schmidt, G. A., and Tausnev, N. *Science* **308**, 1431–1435 (2005).

[26] Trenberth, K. E. and Fasullo, J. T. *J. Climate* **27**, 3129–3144 (2014).

[27] von Schuckmann, K., Palmer, M. D., Trenberth, K. E., Cazenave, A., Chambers, D., Champollion, N., Hansen, J., Josey, S. A., Loeb, N., Mathieu, P.-P., Meyssignac, B., and Wild, M. *Nat. Clim. Change* **6**, 138–144 (2016).

[28] CHENG, L., ABRAHAM, J., ZHU, J., TRENBERTH, K. E., FASULLO, J., BOYER, T., LOCARNINI, R., ZHANG, B., YU, F., WAN, L., CHEN, X., SONG, X., LIU, Y., and MANN, M. E. *Adv. Atmosph. Sci.* **37**, 137–142 (2020).

[29] Steffen, W., Rockström, J., Richardson, K., Lenton, T. M., Folke, C., Liverman, D., Summerhayes, C. P., Barnosky, A. D., Cornell, S. E., Crucifix, M., Donges, J. F., Fetzer, I., Lade, S. J., Scheffer, M., Winkelmann, R., and Schellnhuber, H. J. *PNAS* **33**, 8252–8259 (2018).

[30] Im, E.-S., Pal, J. S., and Eltahir, E. A. B. *Sci. Adv.* **3**, e1603322 (2017).

[31] Burke, M., Hsiang, S. M., and Miguel, E. *Nature* **527**, 235–239 (2015).

[32] Baum, S. D., Denkenberger, D. C., Pearce, J. M., Robock, A., and Winkler, R. *Environ. Syst. Decis.* **35**, 301–313 (2015).

[33] Smith, J., Yeluripati, J., Smith, P., and Nayak, D. R. *Nat. Sustain.* **3**, 247–252 (2020).

[34] *Norwegian Refugee Council (NRC)* (2020).

[35] Mueller, V., Gray, C., and Kosec, K. *Nat. Clim. Change* **4**, 182–185 (2014).

[36] Barnosky, A. D., Hadly, E. A., Bascompte, J., Berlow, E. L., Brown, J. H., Fortelius, M., Getz, W. M., Harte, J., Hastings, A., Marquet, P. A., Martinez, N. D., Mooers, A., Roopnarine, P., Vermeij, G., Williams, J. W., Gillespie, R., Kitzes, J., Marshall, C., Matzke, N., Mindell, D. P., Revilla, E., and Smith, A. B. *Nature* **486**, 52–58 (2012).

[37] Wernberg, T., Bennett, S., Babcock, R. C., de Bettignies, T., Cure, K., Depczynski, M., Dufois, F., Fromont, J., Fulton, C. J., Hovey, R. K., Harvey, E. S., Holmes, T. H., Kendrick, G. A., Radford, B., Santana-Garcon, J., Saunders, B. J., Smale, D. A., Thomsen, M. S., Tuckett, C. A., Tuya, F., Vanderklift, M. A., and Wilson, S. *Science* **353**, 169–172 (2016).

[38] Altizer, S., Ostfeld, R. S., Johnson, P. T. J., Kutz, S., and Harvell, C. D. *Science* **341**, 514–519 (2013).

[39] Ryan, S. J., Carlson, C. J., Mordecai, E. A., and Johnson, L. R. *PLoS Negl. Trop. Dis.* **13**, e0007213 (2019).

[40] Johnson, C. K., Hitchens, P. L., Pandit, P. S., Rushmore, J., Evans, T. S., Young, C. C. W., and Doyle, M. M. *Proc. R. Soc. B* **287**, 20192736 (2020).

[41] Burke, M., González, F., Baylis, P., Heft-Neal, S., Baysan, C., Basu, S., and Hsiang, S. *Nat. Clim. Change* **8**, 723–729 (2018).

[42] Beillouin, D., Schauberger, B., Bastos, A., Ciais, P., and Makowski, D. *Phil. Trans. R. Soc. B* **375**, 110–118 (2020).

[43] Anderson, W. B., Seager, R., Baethgen, W., Cane, M., and You, L. *Sci. Adv.* **5**, eaaw1976 (2019).

[44] Costello, C., Ovando, D., Clavelle, T., Strauss, C. K., Hilborn, R., Melnychuk, M. C., Branch, T. A., Gaines, S. D., Szuwalski, C. S., Cabral, R. B., Rader, D. N., and Leland, A. *PNAS* **113**, 5125–5129 (2016).

[45] Voss, R., Quaas, M. F., Stiasny, M. H., Hänsel, M., Pinto, G. A. S. J., Lehmann, A., Reusch, T. B., and Schmidt, J. O. *J. Environ. Manag.* **238**, 110–118 (2019).

[46] Vasseur, D. A., DeLong, J. P., Gilbert, B., Greig, H. S., Harley, C. D. G., McCann, K. S., Savage, V., Tunney, T. D., and O'Connor, M. I. *Proc. R. Soc. B* **281**, 20132612 (2014).

[47] Pal, J. S. and Eltahir, E. A. B. *Nat. Clim. Change* **6**, 197–200 (2016).

[48] Schiermeier, Q. *Nature* **560**, 20–22 (2018).

[49] Smale, D. A., Wernberg, T., Oliver, E. C. J., Thomsen, M., Harvey, B. P., Straub, S. C., Burrows, M. T., Alexander, L. V., Benthuysen, J. A., Donat, M. G., Feng, M., Hobday, A. J., Holbrook, N. J., Perkins-Kirkpatrick, S. E., Scannell, H. A., Gupta, A. S., Payne, B. L., and Moore, P. J. *Nat. Clim. Change* **9**, 306–312 (2019).

[50] Rodrigues, R. R., Taschetto, A. S., Gupta, A. S., and Foltz, G. R. *Nat. Geosci.* **12**, 620–626 (2019).

[51] Chen, P. and Shakhonovich, E. I. *Biophys. J.* **98**, 1109–1118 (2010).

[52] Huey, R. B., Kearney, M. R., Krockenberger, A., Holtum, J. A. M., Jess, M., and Williams, S. E. *Phil. Trans. R. Soc. B* **367**, 1665–1679 (2012).

[53] Lefevre, S. *Conserv. Physiol.* **4**, cow009 (2016).

[54] Wang, E., Martre, P., Zhao, Z., Ewert, F., Maiorano, A., Rötter, R. P., Kimball, B. A., Ottman, M. J., Wall, G. W., Whitev, J. W., Reynolds, M. P., Alderman, P. D., Aggarwal, P. K., Anothai, J., Basso, B., Biernath, C., Cammarano, D., Challinor, A. J., Sanctis, G. D., Doltra, J., Dumont, B., Fereres, E., Garcia-Vila, M., Gayler, S., Hoogenboom, G., Hunt, L. A., Izaurralde, R. C., Jabloun, M., Jones, C. D., Kersebaum, K. C., Koehler, A.-K., Liu, L., Müller, C., Kumar, S. N., Nendel, C., O'Leary, G., Olesen, J. E., Palosuo, T., Priesack, E., Rezaei, E. E., Ripoche, D., Ruane, A. C., Semenov, M. A., Shcherbak, I., Stöckle, C., Stratonovitch, P., Streck, T., Supit, I., Tao, F., Thorburn, P., Waha, K., Wallach, D., Wang, Z., Wolf, J., Zhu, Y., and Asseng, S. *Nat. Plants* **3**, 17102 (2017).

[55] Pinsky, M. L., Eikeset, A. M., McCauley, D. J., Payne, J. L., and Sunday, J. M. *Nature* **569**, 108–111 (2019).

[56] Sinclair, B. J., Marshall, K. E., Sewell, M. A., Levesque, D. L., Willett, C. S., Slotsbo, S., Helmuth, Y. D. C. D. G. H. D. J. M. B. S., and Huey1, R. B. *Ecol. Lett.* **19**, 1372–1385 (2016).

[57] Nguyen, K. D. T., Morley, S. A., Lai, C.-H., Clark, M. S., Tan, K. S., Bates, A. E., and Peck, L. S. *PLoS ONE* **6**, e29340 (2011).

[58] Panetta, A. M., Stanton, M. L., and Harte, J. *Sci. Adv.* **4: eaaq1819** (2018).

[59] Román-Palacios, C. and Wiens, J. J. *PNAS* **117**, 4211–4217 (2020).

[60] Soroye, P., Newbold, T., and Kerr, J. *Science* **367**, 685–688 (2020).

[61] Sherwood, S. C., Webb, M. J., Annan, J. D., Armour, K. C., Forster, P. M., Hargreaves, J. C., Hegerl, G., Klein, S. A., Marvel, K. D., Rohling, E. J., Watanabe, M., Andrews, T., Braconnot, P., Bretherton, C. S., Foster, G. L., Hausfather, Z., von der Heydt, A. S., Knutti, R., Mauritsen, T., Norris, J. R., Proistosescu, C., Rugenstein, M., Schmidt, G. A., Tokarska, K. B., and Zelinka, M. D. *Rev. Geophys.* **58**, e2019RG000678 (2020).

[62] an Catherine A. Senior, G. A. M., Eyring, V., Flato, G., Lamarque, J.-F., Stouffer, R. J., Taylor, K. E., and Schlund, M. *Sci. Adv.* **6:eaba1981** (2020).

[63] Collins, M., Knutti, R., Arblaster, J., Dufresne, J.-L., Fichefet, T., Friedlingstein, P., Gao, X., Gutowski, W., Johns, T., Krinner, G., Shongwe, M., Tebaldi, C., Weaver, A., and Wehner, M. *Long-term Climate Change: Projections, Commitments and Irreversibility*, book section 12, 1029–1136. Cambridge University Press, Cambridge, United Kingdom and New York, NY, USA (2013).

[64] Myhre, G., Myhre, C. L., Forster, P. M., and Shine, K. P. *Nat. Geosci.* **10**, 710–711 (2017).

[65] Tierney, J. E., Zhu, J., King, J., Malevich, S. B., Hakim, G. J., and Poulsen, C. J. *Nature* **584**, 569–573 (2020).

[66] HANSEN, J., RUSSELL, G., LACIS, A., FUNG, I., RIND, D., and STONE, P. *Science* **229**, 857–859 (1985).

[67] Schwartz, S. E. *J. Geophys. Res.* **112**, D24S05 (2007).

[68] Hansen, J., Sato, M., Ruedy, R., Schmidt, G. A., and Lo, K. (2016).

[69] Oceanic, N. and Administration, A. Accessed November 30th (2020).

[70] Andreae, M. O., Jones, C. D., and Cox, P. M. *Nature* **435**, 1187–1190 (2005).

[71] Myhre, G., Shindell, D., Bréon, F.-M., Collins, W., Fuglestvedt, J., Huang, J., Koch, D., Lamarque, J.-F., Lee, D., Mendoza, B., Nakajima, T., Robock, A., Stephens, G., Takemura, T., and Zhang, H. *Anthropogenic and Natural Radiative Forcing*, book section 8, 659–740. Cambridge University Press, Cambridge, United Kingdom and New York, NY, USA (2013).

[72] Grandey, B. S., Rothenberg, D., Avramov, A., Jin, Q., Lee, H.-H., Liu, X., Lu, Z., Albani, S., and Wang, C. *Atmos. Chem. Phys.* **18**, 15783–15810 (2018).

[73] Bellouin, N., Gryspeerdt, J. Q. E., Kinne, S., Stier, P., Watson-Parris, D., Carslaw, O. B. K. S., , Christensen, M., Daniau, A., Dufresne, J., Feingold, G., Fiedler, S., Forster, P., andv J. M. Haywood, A. G., Lohmann, U., Malavelle, F., Mauritsen, T., McCoy, D. T., Myhre, G., Mülmenstädt, J., Neubauer, D., Possner, A., Rugenstein, M., Sato, Y., Schulz, M., Schwartz, S. E., Sourdeval, O., Storelvmo, T., Toll, V., Winker, D., and Stevens, B. *Rev. Geophys.* **58**, e2019RG000660 (2020).

[74] Samset, B. H., Sand, M., Smith, C. J., Bauer, S. E., Forster, P. M., Fuglestvedt, J. S., Osprey, S., and Schleussner, C.-F. *Geophys. Res. Lett.* **45**, 1020–1029 (2018).

[75] Samset, B. H. *Science* **360**, 148–150 (2018).

[76] Snyder, C. W. *Climatic Change* **156**, 121–138 (2019).

[77] Westervelt, D. M., Mascioli, N. R., Fiore, A. M., Conley, A. J., Lamarque, J.-F., Shindell, D. T., Faluvegi, G., Previdi, M., Correa, G., and Horowitz, L. W. *Atmos. Chem. Phys.* **20**, 3009–3027 (2020).

[78] Ramanathan, V. and Feng, Y. *PNAS* **105**, 14245–14250 (2008).

[79] Samset, B. H., Fuglestvedt, J. S., and Lund, M. T. *Nat. Commun.* **11**, 3261 (2020).

[80] van Heerwaarden, C. C., Mol, W. B., Veerman, M. A., Benedict, I. B., Heusinkveld, B. G., Knap, W. H., Kazadzis, S., Kouremeti, N., and Fiedler, S. **arXiv:2008.13497** (2020).

[81] Rothman, D. H. *Sci. Adv.* **3**, e1700906 (2017).

[82] Hansen, J., Sato, M., Kharecha, P., von Schuckmann, K., Beerling, D. J., Cao, J., Marcott, S., Masson-Delmotte, V., Prather, M. J., Rohling, E. J., Shakun, J., Smith, P., Lacis, A., Russell, G., and Ruedy, R. *Earth Syst. Dynam.* **8**, 577–616 (2017).

[83] Lenton, T. M., Rockström, J., Gaffney, O., Rahmstorf, S., Richardson, K., Steffen, W., and Schellnhuber, H. J. *Nature* **592**, 575–595 (2019).

[84] Pistone, K., Eisenman, I., and Ramanathan, V. *Gephys. Res. Lett.* **46**, 7474–7480 (2019).

[85] Randers, J. and Goluke, U. *Sci. Rep.* **10**, 18456 (2020).

[86] Greenough, C. F. Master's thesis, Plymouth State University, 5 (2017). Master's thesis.

[87] Roddis, P., Carver, S., Dallimer, M., Norman, P., and Ziv, G. *Appl. Energy* **226**, 353–364 (2018).